Neuropharmacology 186 (2021) 108467

Contents lists available at ScienceDirect

Neuropharmacology

journal homepage: www.elsevier.com/locate/neuropharm

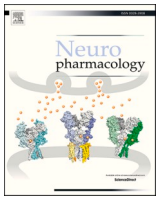

Exposure of R6/2 mice in an enriched environment augments P42 therapy efficacy on Huntington's disease progression

Simon Couly [a,1], Allison Carles [a], Morgane Denus [a], Lorraine Benigno-Anton [b], Florence Maschat [a,**], Tangui Maurice [a,*]

[a] MMDN, Univ Montpellier, EPHE, INSERM, Montpellier, France
[b] Medesis Pharma, Baillargues, France

ARTICLE INFO

Keywords:
Huntington's disease
R6/2 mice
P42 peptide
Hamlet test
Environmental enrichment
BDNF

ABSTRACT

Huntington's disease (HD) is due to a mutation in the gene encoding for Huntingtin protein generating polyQ domain extension. Mutant Htt (mHtt) leads to important dysfunction of the BDNF/TrkB signaling. We previously described the 23aa Htt fragment P42, that attenuated the pathological phenotypes induced by mHtt. We reported that, in the R6/2 mouse model of HD, P42 rescued striatal TrkB level but marginally increased cortical BDNF. In the present study, our aim was to address P42 neuroprotection in presence of an external input of BDNF. We combined P42 administration with environmental enrichment (EE), induced by training in the Hamlet test. We examined the consequences of P42 + EE combination on different phenotypes in R6/2 HD mice: motor and cognitive performances, recorded at early and late pathological stages, and analyzed aggregated mHtt and BDNF levels in forebrain structures. Hamlet exploration (*i.e.*, entries in Run, Hide, Eat, Drink and Interact houses) was gradually impaired in R6/2 mice, but maintained by P42 treatment until week 8. Topographic memory alteration measured at week 7 was attenuated by P42. Motor performances (rotarod) were significantly ameliorated by the P42 + EE combination until late stage (week 12). The P42 + EE combination also significantly decreased aggregated Htt levels in the hippocampus, striatum and cortex, and increased BDNF levels in the cortex and striatum. We concluded that combination between P42 treatment, known to increase TrkB striatal expression, and a BDNF-enhancing therapy such as EE efficiently delayed HD pathology in R6/2 mice. Use of dual therapies might be a pertinent strategy to fight neurodegeneration in HD.

1. Introduction

Huntington disease (HD) is an autosomal, dominantly inherited neurodegenerative disease, caused by an expansion of cytosine–adenine–guanine (CAG) repeats in the first exon of the huntingtin gene, which encodes the Huntingtin (Htt) protein (Dorsey et al., 2013). The inherited mutation results in production of an elongated polyQ mutant Huntingtin (mHtt) protein. The expansion of CAG repeats leads to the formation of intracellular and intranuclear aggregates in affected neurons (Orr et al., 1993). HD patients develop severe mental and physical disabilities due to brain atrophy and loss of neurons in the striatum and cerebral cortex (Huntington, 1872). Htt protein is expressed in most tissues and is involved in protein trafficking, postsynaptic signaling, vesicle transport, transcriptional regulation and regulation of cell death. Accumulation of mHtt variant results in alteration of gene transcription, energy production, dysregulation of neurotransmitter metabolism, and activation of intracellular pathways, particularly those leading to endoplasmic reticulum (ER) stress (Reijonen et al., 2008). Moreover, mHtt provokes a dysfunction of the brain-derived neurotrophic factor (BDNF) neurotrophin system, particularly affecting its high-affinity receptor TrkB associated signaling pathway (Ginés et al., 2006; Gharami et al., 2008; Giralt et al., 2009). Indeed, mHtt reduces levels of BDNF in the striatum, likely by inhibiting cortical *bdnf* gene expression and the anterograde transport of BDNF from the cortex to the striatum. A specific reduction of TrkB receptors was measured in transgenic exon-1 and full-length knock-in HD mouse models and in the motor cortex and

* Corresponding author. MMDN, INSERM UMR_S1198, University of Montpellier, CC105, Place Eugène Bataillon, 34095, Montpellier cedex 5, France.
** Corresponding author. MMDN, INSERM UMR_S1198, University of Montpellier, CC105, Place Eugène Bataillon, 34095, Montpellier cedex 5, France.
E-mail addresses: florence.maschat@umontpellier.fr (F. Maschat), tangui.maurice@umontpellier.fr (T. Maurice).
[1] **Present address:** Cellular Pathobiology Section, Integrative Neuroscience Research Branch, Intramural Research Program, National Institute on Drug Abuse, NIH, 333 Cassell Drive, Baltimore, MD 21224, USA.

https://doi.org/10.1016/j.neuropharm.2021.108467
Received 11 November 2020; Received in revised form 11 January 2021; Accepted 14 January 2021
Available online 28 January 2021

caudate nucleus of HD patient brains (Ginés et al., 2006). Alterations of BDNF expression has been also observed in mouse models of HD. In the R6/2 line, reduction seems however variable depending on the studies, either found unchanged (Bobrowska et al., 2011; Nguyen et al., 2016) or reduced in the cortex and striatum (Luthi-Carter et al., 2002; Couly et al., 2018). Reduced BDNF level largely influences striatal deficit that is associated with motor impairment (Canals et al., 2004) and neuropathology in HD (Strand et al., 2007). BDNF neurotrophic support in striatum may result from impaired axonal transport machinery (Gauthier et al., 2004) or altered TrkB receptor signal transduction (Plotkin et al., 2014). The effectiveness of BDNF also depends on its receptor TrkB whose mRNA and protein levels deficits were also reported in HD striatal cells and human patients (Ginés et al., 2006). Therefore, neurotrophin-based therapies for HD should address both the deficit in BDNF supply (Bates et al., 2015) and the impaired signal transduction from the TrkB receptor (Apostol et al., 2008; Simmons et al., 2013).

We previously described P42, a 23aa peptide isolated from endogenous Htt, within a region rich in proteolytic sites, that plays a critical role in pathogenesis. We showed that P42 is able to improve several of the pathological phenotypes induced by mHtt. P42-induced neuroprotection was first demonstrated using a Drosophila model of HD on mHtt aggregation, on different polyQ-hHtt induced neuronal phenotypes including eye degeneration or impairment of vesicular axonal trafficking, and on physiological behaviors such as larval locomotion and adult survival (Arribat et al., 2013). The therapeutic potential of P42 was then confirmed in a murine model of the disease, the R6/2 mouse. To deliver P42, an original strategy was developed combining the properties of the cell penetrating peptide TAT from HIV and a nanostructure-based drug delivery system, the Aonys® technology (Medesis Pharma), to form a water-in-oil microemulsion allowing non-invasive per mucosal buccal/rectal administration (Arribat et al., 2014). P42 was effectively delivered into the brain and targeted most cells, including striatal neurons. It allowed a clear improvement of HD-associated behavioral defects such as foot-clasping, falling latency in the rotarod and body weight, and of several histological markers of HD on brain slices such as aggregation, astrogliosis or enlargement of ventricular areas (Arribat et al., 2014). More recently, we reported the P42 mechanism of action on BDNF/TrkB pathway in R6/2 mice. P42 partially restored TrkB protein level in the striatum and attenuated the diminution of *bdnf* transcript level in the cortex (Couly et al., 2018). As a consequence, P42 treatment ameliorated BDNF/TrkB associated behavioral deficits in R6/2 mice, such as memory, anxiety and motor coordination (Couly et al., 2018).

Since P42 is essentially acting on TrkB level of expression in the striatum, we asked whether enhancing BDNF will increase P42 efficiency. An effective strategy to enhance BDNF levels in forebrain structures can be achieved by environmental enrichment (EE) (Falkenberg et al., 1992; Bekinschtein et al., 2011). In particular, beneficial effects of increased BDNF level gained through EE have been described in several pathological conditions such as chemically-induced seizures (Young et al., 1999; Guilarte et al., 2003), stroke (Zhao et al., 2001), or HD (Spires et al., 2004).

In order to analyze the impact of a BDNF increase on the efficacy of P42, we used in the present study a therapeutic strategy combining P42 and EE. EE was induced using a novel behavioral procedure, the Hamlet test (Crouzier et al., 2018, 2020; Crouzier and Maurice, 2018). In this test, animals are long-lastingly placed in a wider and more ecological space composed of different houses functionalized for basic ethological functions such as running, drinking, eating, hiding and interacting. Maze exploration, topographic memory and the impact of EE on pathology were evaluated. The results showed that combination of P42 treatment and EE indeed maintained BDNF levels, even at a late stage of the pathology, and markedly potentiated motor and memory performances of HD mice.

Table 1
Experimental groups.

Genotype:		WT		R6/2	
Treatment:		V	P42	V	P42
Female	NT	17	6	6	9
Female	T	9	9	13	12
Male	NT	16	6	8	7
Male	T	8	6	9	13

2. Material and methods

2.1. Peptide synthesis and formulation

To ensure P42 diffusion, we designed a fusion peptide where P42, a 23 amino-acids peptide, was conjugated to the 11 amino-acids TAT cell penetrating peptide (YGRKKRRQRRR). The fusion peptide P42TAT (AASSGVSTPGSAGHDIITEQPRS-GG-YGRKKRRQRRR) was synthetized and purified (>95%) by GenScript (Piscataway, NJ, USA). P42TAT was then diluted in water and mixed with a lipid mixture (Aonys® technology, Medesis Pharma, Baillargues, France), composed of self-assembled specific polar lipids, surfactant and co-surfactants lecithin and ethanol, with a final water content of 12%. After a few seconds of vortexing a water-in-oil (*i.e.*, reverse) microemulsion was formed. These microemulsions meet the criteria of a Newtonian fluid that is limpid and isotropic (Mouri et al., 2014, 2015, 2016). Aonys® microemulsions are designed for administration of active pharmaceutical ingredients, referred here as P42 treatment, via application to the buccal and rectal mucosa of the mouse.

2.2. R6/2 transgenic mice, experimental cohorts and P42 treatment

The R6/2 mouse model is based on the expression of the polyQ expanded human exon 1 and shows early and strong HD symptoms, leading to a premature death at 3 months of age. Heterozygous R6/2 males were obtained from Jackson Laboratory (stock 006494) and were crossed with C57BL/6-CBA wildtype (WT) females (Janvier, St-Berthevin, France). Mice were genotyped by PCR using tail-tip DNA with the primers 5′-CGGCTGAGGCAGCAGCGGCTGT-3’ (sens) and 5′-GCAGCAGCAGCAGCAACAGCCGCCACCGCC-3’ (antisens). Mice were housed in the animal facility of the University of Montpellier (CECEMA; registration number E34-172-13). Animals were housed in groups with access to food and water *ad libitum*. They were kept in a temperature and humidity controlled facility on a 12-h/12-h light/dark cycle with light on at 7:00 a.m. All animal procedures were conducted in strict adherence to the European Union Directive 2010/63 and the ARRIVE guidelines (Kilkenny et al., 2010).

Cohorts analyzed included WT and R6/2 mice, trained or not in the Hamlet and treated with empty Aonys® microemulsion (Vehicle, V) or with P42TAT-Aonys® microemulsions (P42, 1.2 mg/kg). The number of animals per group and per cohort is detailed in Table 1. Treatments were administered via buccal and rectal mucosa deposits, five days a week, at 9:00 a.m., in a volume of 1 mL/kg. Littermates were treated with P42 from week 4 until sacrifice, *i.e.*, week 11–12 (Fig. 1a). Body weights were measured twice a week to check the general condition of the mice. No drastic loss of weight has been observed during the time of the experimentation (Supplemental Fig. 1).

Mice were trained in the Hamlet on weeks 5–6 or on weeks 8–9, in order to analyze the EE impact on early and late stages of the pathology (Fig. 1a). Motor performance were tested in the rotarod 5 days and 19 days after training end, thus on weeks 7 and 9 for the first batch (Batch 1) and on weeks 10 and 12 for the second (Batch 2) (Fig. 1a). Mice were sacrificed at week 11 or 12 as indicated and brain structures were dissected and frozen for post-mortem analyses.

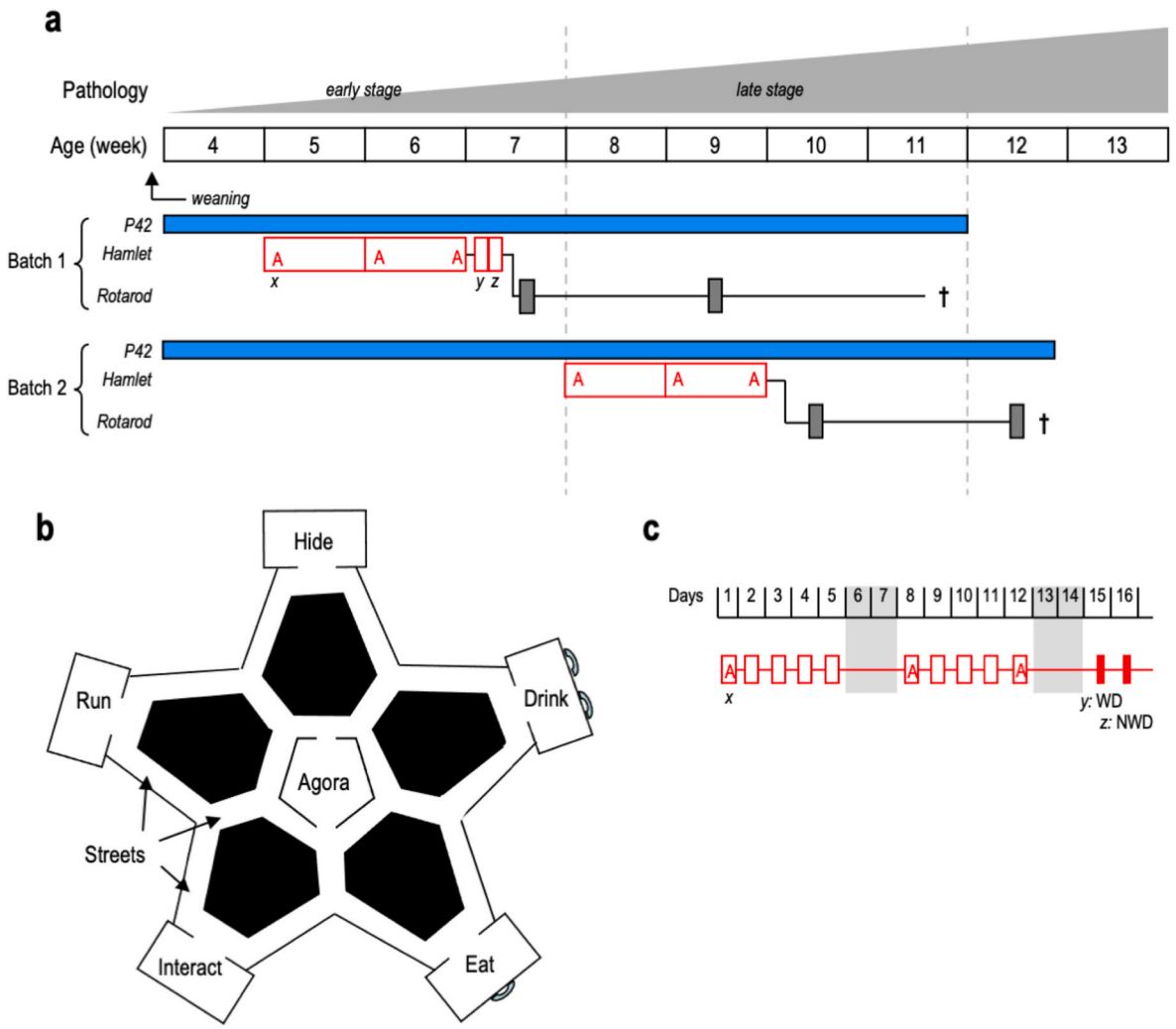

Fig. 1. (**a**) Experimental design and timeline. Huntington's pathology evolves rapidly in R6/2 mice between 4 and 13 weeks of age. P42 treatment started after weaning at 4 weeks of age and was continued until sacrifice. Training in the Hamlet was done either at an early stage of the disease, between 5 and 7 weeks of age for batch 1, or at a late stage of the disease, between 8 and 10 weeks of age for batch 2. (**b**) Hamlet map showing the houses, central agora and streets. (**c**) In more details training (indicated by *x*) consisted in 4 h/day (red rectangles) in the Hamlet during two weeks. Topographic memory was analyzed for animals of the first batch, 72 h after the last training session for their ability to find the Drink house in water-deprived (WD) condition (indicated by *y*) and in non-water-deprived (NWD) condition (indicated by *z*). The Rotarod test was performed at weeks 7, 9, 10 and 12. Training days analyzed (days 1, 6 and 10 of the training period) are indicated by *A* in (a, c); sacrifices are indicated by †.

2.3. Training in the hamlet and measure of topographic memory

The Hamlet (diameter 1.2 m) was designed in the laboratory but elaborated by Viewpoint (Lissieu, France). It has a single level, 50 cm above the floor, with an agora at its center and streets expanding in a star shape towards five functionalized compartments, called houses (Fig. 1b). The walls and walkways are made of IR-transparent polyvinyle chloride. The room was uniformly illuminated (200 Lux). Infra-red emitting diodes are placed under the floor and an IR sensitive camera captures the animal behavior. The agora served as a gathering area and as a start box for training and test trials. The functionalized houses contained pellets (physiological function encoded: Eat), water (Drink), a novomaze (Viewpoint) (Hide), a running wheel (Run) or a grid isolating a stranger mouse (Interact). Procedures and protocols have been previously described in details (Crouzier et al., 2018, 2020; Crouzier and Maurice, 2018). In brief, animals were placed in the Hamlet in groups (WT or R6/2 animals from the same housing cage) for 4 h per day during the 2-weeks training periods (Fig. 1c). A global activity index was determined from the measure of the time, in sec, of occupation of the five houses divided by the number of mice in the hamlet for each hour during the 4 h of a training session. The exploration profiles in the Hamlet was analyzed in days 1, 6 and 10, corresponding to the beginning, middle and end of the training period (Fig. 1c). The topographic memory was evaluated 72 h after the last training session in mice from the first batch, using a probe test (Crouzier and Maurice, 2018). The probe test consisted in measuring the ability of mice to orientate in the maze and find the Drink house under normal or water-deprived condition: thirsty mice run faster from the agora to the Drink house when they show a better topographic memory (Crouzier et al. 2018, 2020). In brief, animals were placed individually in the agora and free to explore the Hamlet during a 10-min session and the exploratory behavior was videotracked (Viewpoint) and analyzed in terms of latency to reach the goal and other houses and number of errors (entries into a street not directing to the goal house). Two sessions were performed at 24 h interval: first, in water-deprived (WD) condition and, then, in non-water deprived condition (NWD) (Fig. 1c). WD consisted in removing the drinking bottle from the housing cage, 15 h before the probe test.

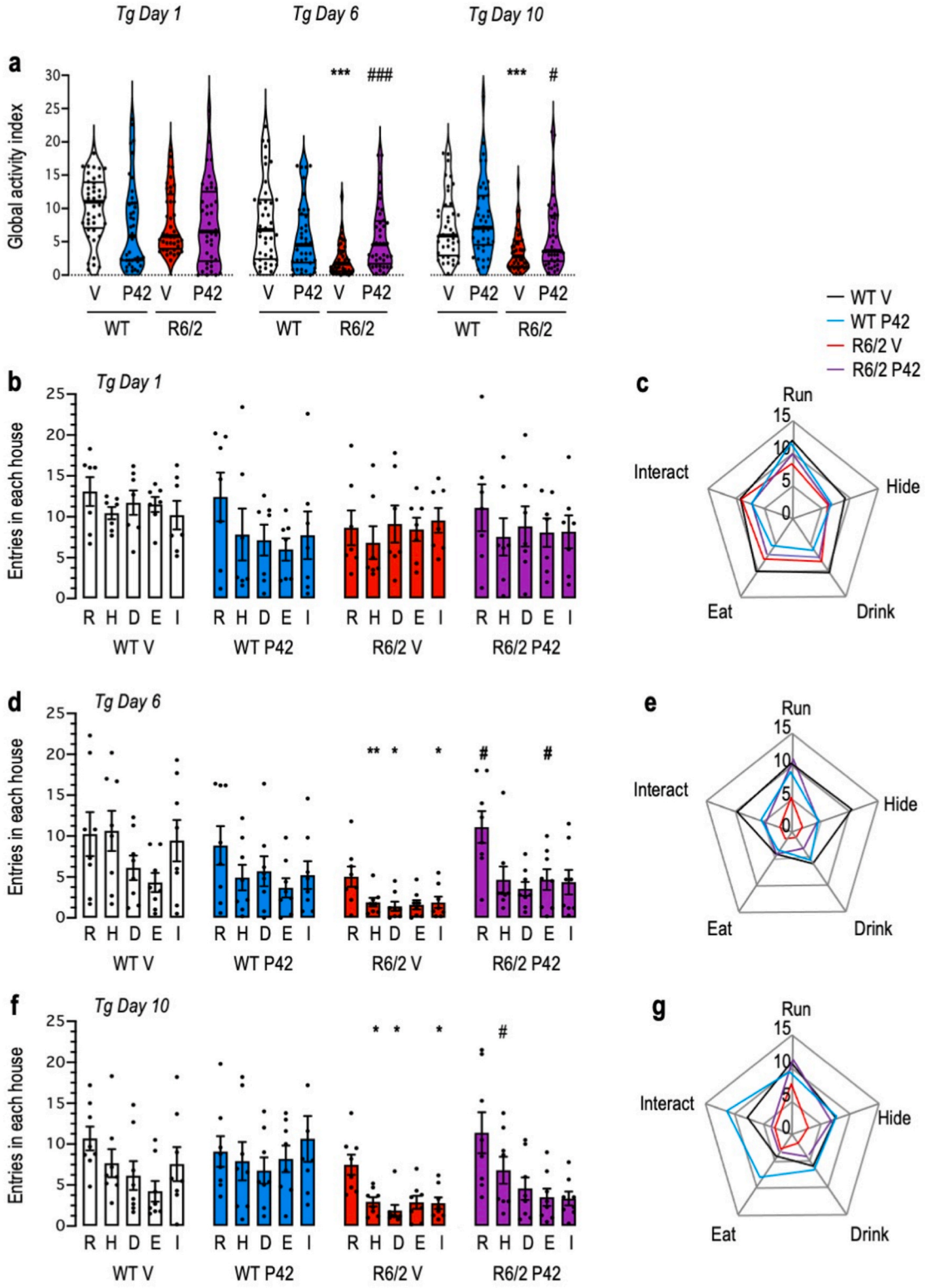

Fig. 2. Analysis of the activity of 5-6-week old R6/2 mice during training in the Hamlet. (**a**) Global and (**b-g**) detailed activity in the houses measured during training day 1 (b, c), day 6 (d, e) and day 10 (f, g), *i.e.*, at the beginning, middle and end of the training period. Data are also shown as radar graphs (c, e, g). Abbreviations: Tg Day, training day; WT, wildtype; V, vehicle solution; R, Run house; H, Hide house; D, Drink house; E, Eat house; I, Interact house. Two-way ANOVA in (a): on day 1, $F_{(1,28)} = 1.198$, $p = 0.2831$ for the genotype, $F_{(1,28)} = 2.695$, $p = 0.1119$ for the treatment and $F_{(1,28)} = 1.7325$, $p = 0.1998$ for the interaction; on day 6, $F_{(1,28)} = 13.79$, $p = 0.0009$ for the genotype, $F_{(1,28)} = 0.2623$, $p = 0.6126$ for the treatment and $F_{(1,28)} = 13.79$, $p = 0.0009$ for the interaction; on day 10, $F_{(1,28)} = 16.96$, $p = 0.0003$ for the genotype, $F_{(1,28)} = 5.235$, $p = 0.0299$ for the treatment and $F_{(1,28)} = 0.5171$, $p = 0.4780$ for the interaction. At day 6 and day 10, R6/2 present significant deficits in their activity and P42 is able to rescue these deficits. $^{*}p < 0.05$, $^{**}p < 0.01$, $^{***}p < 0.001$ *vs.* V-treated WT group; $\#p < 0.05$, $\#\#\#p < 0.001$ *vs.* V-treated R6/2 group; Mann-Whitney's test.

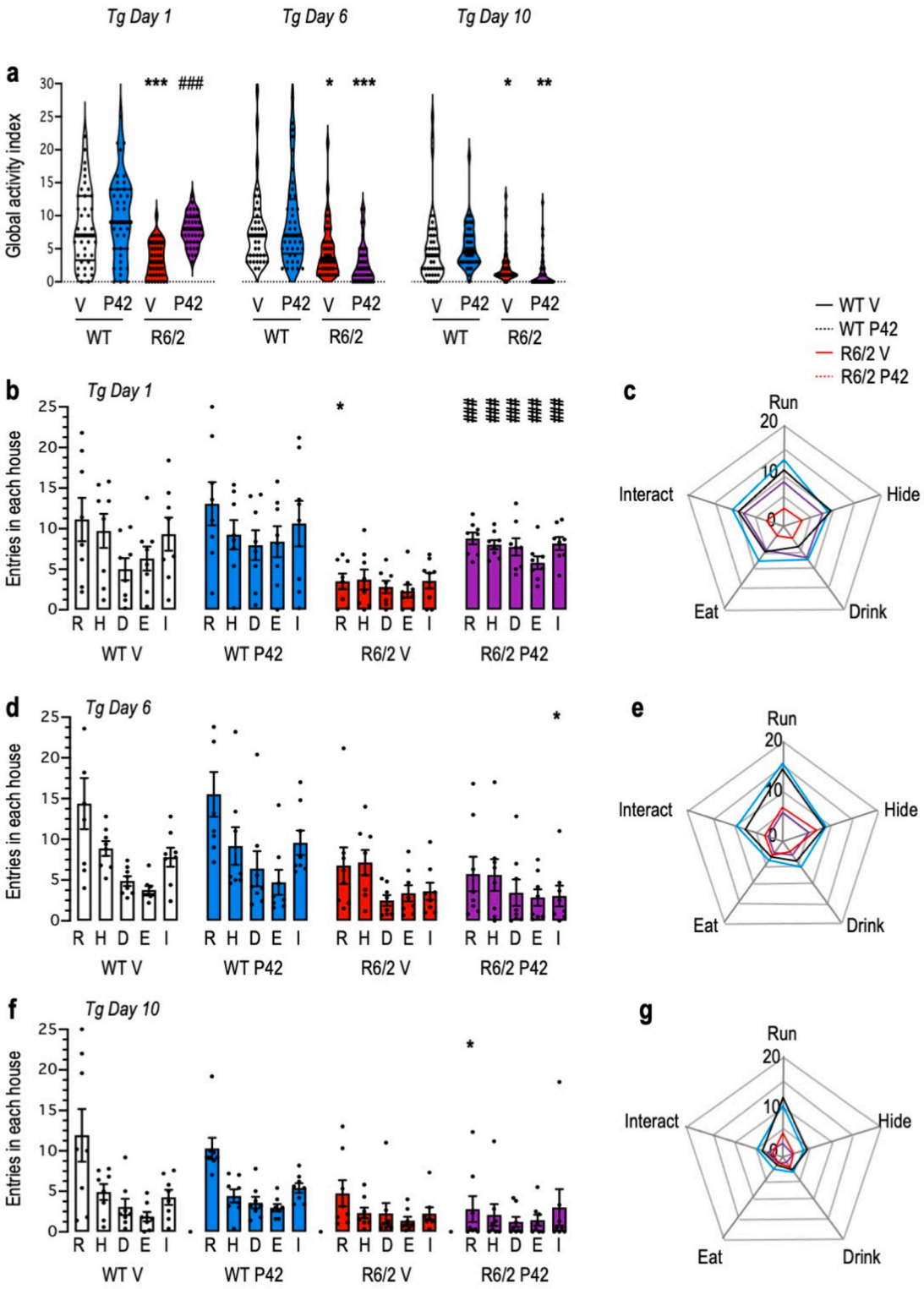

Fig. 3. Analysis of the activity of 8-9-week old R6/2 mice during training in the Hamlet. (**a**) Global and (**b-g**) detailed activity in the houses measured during training day 1 (b, c), day 6 (d, e) and day 10 (f, g), *i.e.*, at the beginning, middle and end of the training period. Data are also shown as radar graphs (c, e, g). Abbreviations: Tg Day, training day; WT, wildtype; V, vehicle solution; R, Run house; H, Hide house; D, Drink house; E, Eat house; I, Interact house. Two-way ANOVA in (a): on day 1, $F_{(1,28)} = 24.45$, $p < 0.0001$ for the genotype, $F_{(1,28)} = 17.17$, $p = 0.0003$ for the treatment and $F_{(1,28)} = 4.043$, $p = 0.0541$ for the interaction; on day 6, $F_{(1,28)} = 22.84$, $p < 0.0001$ for the genotype, $F_{(1,28)} = 0.1267$, $p = 0.7245$ for the treatment and $F_{(1,28)} = 0.9497$, $p = 0.3381$ for the interaction; on day 10, $F_{(1,28)} = 19.61$, $p = 0.001$ for the genotype, $F_{(1,28)} = 0.075$, $p = 0.7862$ for the treatment and $F_{(1,28)} = 0.2225$, $p = 0.6408$ for the interaction. *$p < 0.05$, **$p < 0.01$, ***$p < 0.001$ *vs.* V-treated WT group; #$p < 0.05$, ###$p < 0.001$ *vs.* V-treated R6/2 group; Mann-Whitney's test.

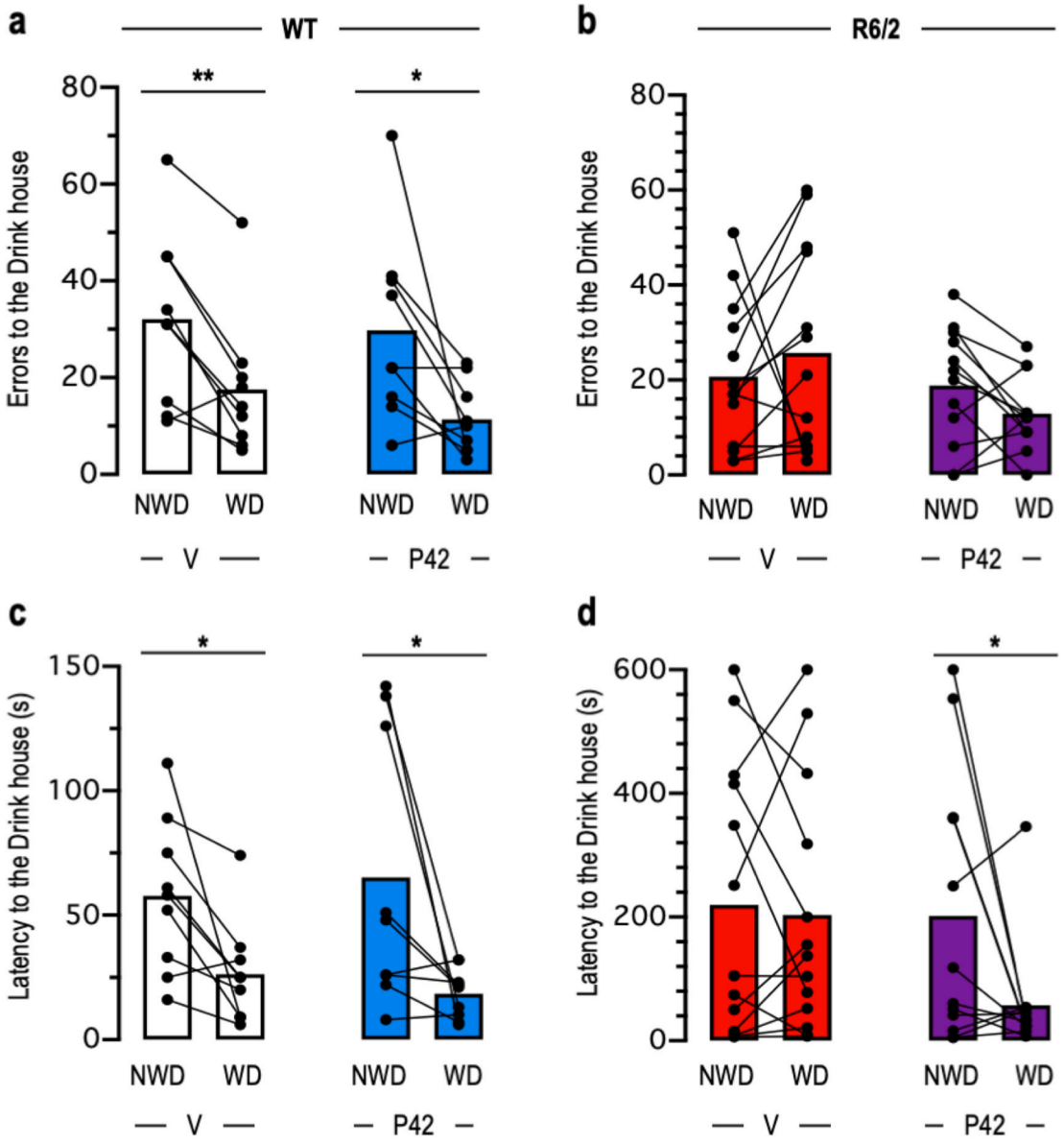

Fig. 4. Analysis of topographic memory in 7-week old R6/2 mice in the Hamlet. Mice were tested in water deprived (WD) condition 72 h after the last training session and after 24 h in non-water deprived (NWD) condition. (a, b) Number of errors and (c, d) latencies spent to reach the Drink house for WT (a, c) and R6/2 mice (b, d). Two-way ANOVA: $F_{(1,32)} = 10.78$, $p = 0.0025$ for the condition, $F_{(1,32)} = 0.802$, $p = 0.3772$ for the treatment and $F_{(1,32)} = 0.2475$, $p = 0.6222$ for the interaction in (a); $F_{(1,32)} = 6.496$, $p = 0.0158$ for the condition, $F_{(1,32)} = 0.1155$, $p = 0.7362$ for the treatment and $F_{(1,32)} = 0.5421$, $p = 0.4669$ interaction in (b); $F_{(1,46)} = 0.218$, $p = 0.6428$ for the condition and $F_{(1,46)} = 0.6056$, $p = 0.4404$ for the treatment, $F_{(1,46)} = 2.931$, $p = 0.0936$ for the interaction in (c); $F_{(1,46)} = 2.204$, $p = 0.045$ for the condition, $F_{(1,46)} = 2.259$, $p = 0.1397$ for the treatment and $F_{(1,46)} = 1.376$, $p = 0.2468$ for the interaction in (d).*$p < 0.05$, **$p < 0.01$ *vs.* NWD group; paired *t*-test.

2.4. Motor performance analyses using the rotarod test

Motor performance was assessed using an accelerating rotarod (Stoelting, Ugo Basile, Varese, Italy) twice for each animal group at 2 weeks interval. On the first day, the mice were trained with a trial at an accelerating velocity from 4.5 to 40 rpm. Subsequently, two trials were performed during two consecutive days. In each trial, mice were placed onto the rotarod at a constant speed of 4.5 rpm for 5 s, which then accelerated at a constant rate up until 40 rpm, for a maximum of 5 min. The daily trial was composed of two sessions of 5 min separated by 5–20 min. The latency to fall from the rotarod was recorded every day for each mouse, and the average of the two last trials was used for statistical analysis.

2.5. Western blot analyses

Different areas of mouse brains were dissected and frozen. Samples were homogenized on ice in lysis buffer (100 mM Tris-HCl pH 7.2, 400 mM NaCl, 4 mM ethylenediaminetetraacetic acid (EDTA), 0.2% Triton, 0.05% NaN_3, 0.5% gelatin, 1 mM phenylmethylsulfonyl fluoride (PMSF), Complete™, anti-protease cocktail 25× (Mini, EDTA-free, Sigma-Aldrich). After a 10 min centrifugation at 15 000 *g* at 4 °C, supernatants were collected and protein concentrations assessed. Protein contents were quantified with BCA protein assay kit (Pierce). Total proteins (50 μg) were diluted in sodium dodecyl sulfate loading buffer. Samples were loaded in 4–15% polyacrylamide resolving gel (Mini-Protean® TGX Stain-Free™ precast gels, Bio-Rad) and electroblotted onto 20 μm nitrocellulose membrane (Amersham Protran™ 0.2 NC supported western blotting membranes, GE Healthcare). Blots were

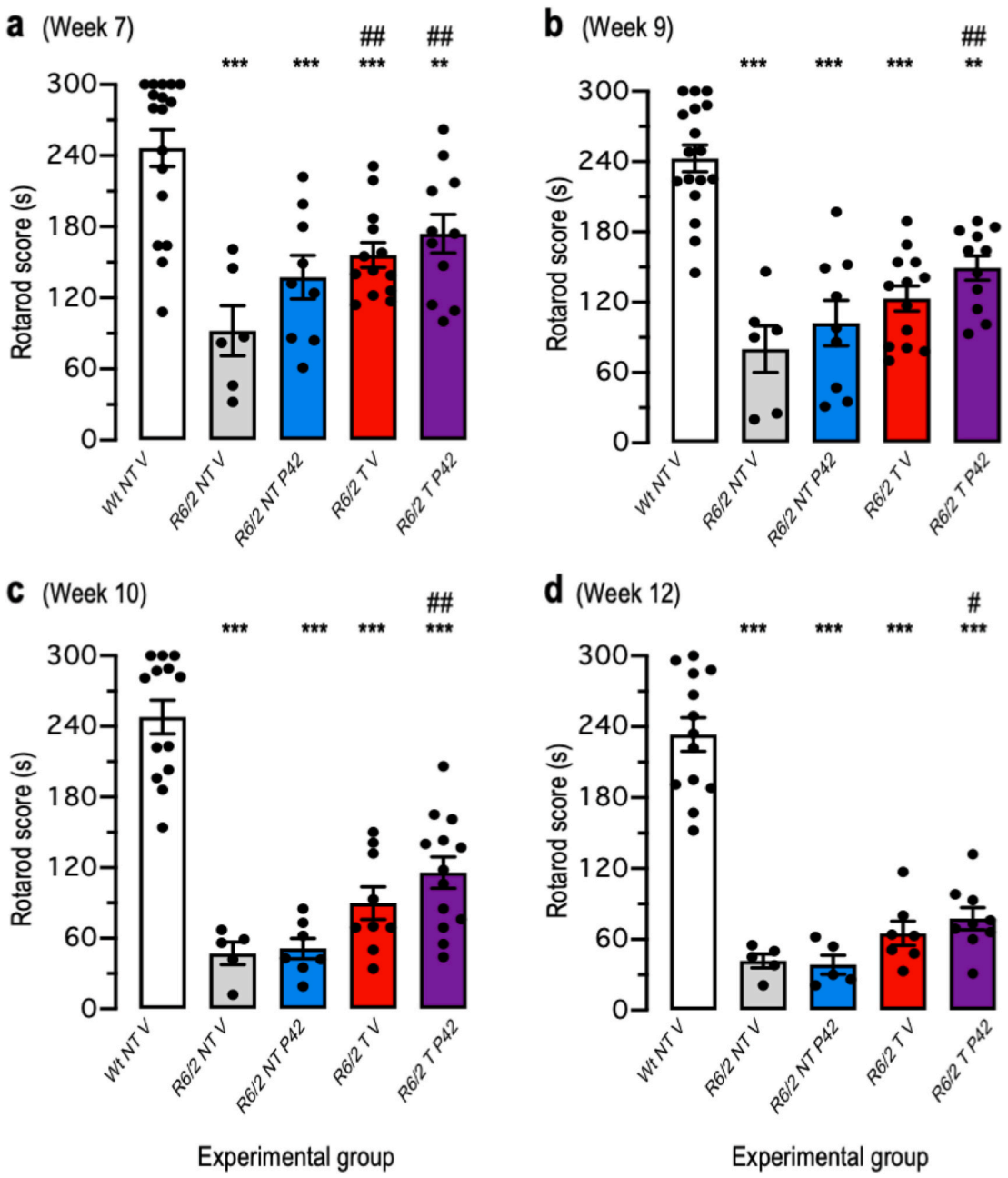

Fig. 5. Performances of WT and R6/2 mice in the Rotarod test after P42 treatment and/or training in the Hamlet. Mice were tested at week 7 (a), 9 (b), 10 (c), and 12 (d). Abbreviations: V, vehicle solution; T, trained; NT, non-trained. ANOVA: $F_{(4,55)} = 12.31$, $p < 0.0001$, in (a); $F_{(4,55)} = 24.72$, $p < 0.0001$, in (b); $F_{(4,46)} = 36.46$, $p < 0.0001$, in (c); $F_{(4,38)} = 50.99$, $p < 0.0001$, in (d). $^{**}p < 0.01$, $^{***}p < 0.001$ *vs*. WT NT V group; $\#p < 0.05$, $\#\#p < 0.01$ *vs*. R6/2 NT V group; Dunnett's test.

blocked in phosphate buffer saline (PBS) containing 0.1% Tween-20 (PBS-T) and 5% non-fat dry milk for 30 min and incubated with primary antibodies overnight at 4 °C. Primary antibodies used were MAB5374 for Htt (1:200; Merck) and AB1534 (1:500; Merck) for BDNF. After 3 washes of 5 min with PBS-T, membranes were incubated 1 h with horseradish peroxidase-conjugated anti-rabbit antibody 111-035-144 (1:10 000; Jackson Immunoresearch) or anti-mousse antibody 100-152-89 (1:10 000; Jackson Immunoresearch), then washed 3 times for 10 min. To visualize the signal, blots were incubated in Clarity™ Western enhanced chemiluminescence substrate (Bio-Rad) during 5 min. Pictures of the chemioluminescence signals were taken with Chemidoc System (Bio-Rad). Normalization was performed with the total protein using Stain-Free™ system. Stain-free technology eliminated many of the issues related to signal normalization for accurate protein quantitation. Total protein level was directly measured on the gel used for western blotting. The total density for each lane was measured without need to strip and reprobe blots for housekeeping proteins to normalize protein levels but rather by using the total lane profile (Gilda and Gomes 2013; Gürtler et al., 2013).

2.6. Statistical analyses

Data were presented as mean ± SEM and analyzed by one-way or two-way analyses of variance (ANOVA, F value), followed by Dunnett's or Newmann-Keuls multiple comparison test. For reading clarity, all statistical data were included in the legend of the figures.

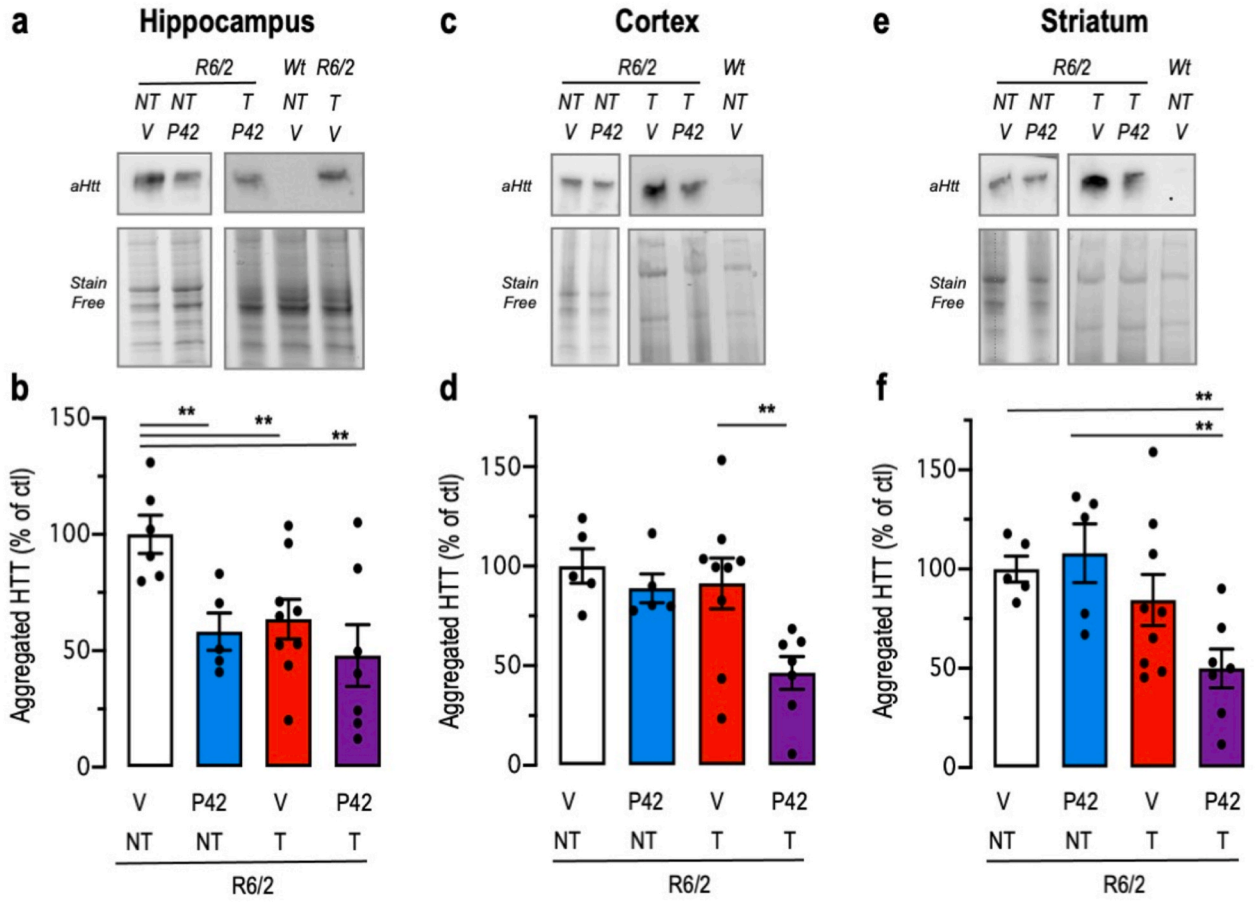

Fig. 6. Effect of the P42 treatment or/and training in the Hamlet on R6/2 mouse brain levels of aggregated Htt, in the hippocampus (a, b), cortex (c, d) and striatum (e, f). Upper panels (a, c, e) show typical aggregated Htt (aHtt) and stain free blots. Lower panels (d, d, f) show quantification in each structure. Abbreviations: WT, wild-type; NT, non-trained; T, trained; V, vehicle solution. Two-way ANOVA: $F_{(1,29)} = 8.906$, $p = 0.0057$ for the treatment, $F_{(1,29)} = 5.829$, $p = 0.0223$ for the training, $F_{(1,29)} = 1.843$, $p = 0.1851$ for the interaction in (b); $F_{(1,20)} = 4.857$ $p = 0.0394$ for the treatment, $F_{(1,20)} = 5.156$, $p = 0.0344$ for the training, $F_{(1,20)} = 1.61$, $p = 0.219$ for the interaction in (d); $F_{(1,22)} = 1.121$, $p = 0.3013$ for the treatment, $F_{(1,22)} = 8.667$, $p = 0.0075$ for the training, $F_{(1,22)} = 2.882$, $p = 0.1037$ for the interaction in (f). $^{**}p < 0.01$; Newman-Keuls test.

3. Results

3.1. Hamlet training of R6/2 mice, treated or not with P42 peptide

The P42 treatment was begun at week 4 of age and pursued until sacrifice. EE was induced by a 2-weeks training in the Hamlet. The combination P42 + EE was therefore analyzed at two stages of the HD pathology in the R6/2 HD mouse line, *i.e.*, an early stage between weeks 5–6 for the mouse batch 1, and a late stage between weeks 8–9 for batch 2 (Fig. 1a). The general exploration of the houses, leading to an index of mice activity during the training session was analyzed for days 1, 6 and 10, *i.e.*, at the beginning, middle and end of the training period (Figs. 2 and 3). For batch 1, the global activity index, presented as violin graphs, showed no difference among groups in day 1, but rapidly V-treated R6/2 mice showed decreased activity in the Hamlet comparative to WT ($p < 0.001$), at days 6 and 10 (Fig. 2a). The P42 treatment prevented the decrease in activity observed for R6/2 mice with a significant effect on treatment and interaction between gentotype and treatment in days 6 ($p < 0.001$) and 10 ($p < 0.05$) (Fig. 2a). Analysis of the activity in each house showed that all houses were actively explored during day 1, whatever the group (Fig. 2b). The radar graph representation indeed showed overlapping, regular pentagonal signature for all groups (Fig. 2c). During days 6 and 10, a preferential activity in the Run, Hide and Interact houses was noted in V- or P42-treated WT mice (Fig. 2d,f). V-treated R6/2 mice showed marked decreases in all houses, whereas maintaining a preferential activity in the Run house (Fig. 2d,f). The P42 treatment increased activity levels in all houses, with the maintenance of the preferential presence in the Run house. The radar graphs clearly illustrated that V-treated R6/2 mice presented a narrowing of the signature, while the P42 treatment maintained it close to the WT mice trace (Fig. 2e,g).

For mice from batch 2, the global activity index showed that V-treated R6/2 mice presented a decreased activity in the Hamlet, at all training day analyzed (Fig. 3a). The P42 treatment prevented the decrease in activity observed for R6/2 mice with a significant treatment effect in day 1 only, but with no effect in days 6 and 10 (Fig. 3a). Analysis of the activity in each house showed a preferential activity in the Run house and in a lesser extent in the Hide and Interact houses for V- or P42-treated WT mice in all training days (Fig. 3b,d,f). V-treated R6/2 mice showed marked decreases in all houses and the P42 treatment increased activity levels in all houses during training day 1 (Fig. 3b), but not at later timing (Fig. 3d,f). The radar graphs clearly illustrated that the P42 treatment did not affect the signatures as compared to V-treated WT mice at any of the training days analyzed. V-treated R6/2 mice presented a narrowing of the signature at all training day. Finally, the P42 treatment enlarged the signature in day 1 but was without effect at later timing (Fig. 3c,e,g).

Topographic memory was tested in mice from batch 1 (Fig. 4), as they were 7 weeks-old at the end of training in the Hamlet. Data are presented as number of errors (Fig. 4a and b) and latency spent to reach the goal house (Fig. 4c and d). Both V-treated and P42-treated WT groups showed significant reductions of both errors and latencies when

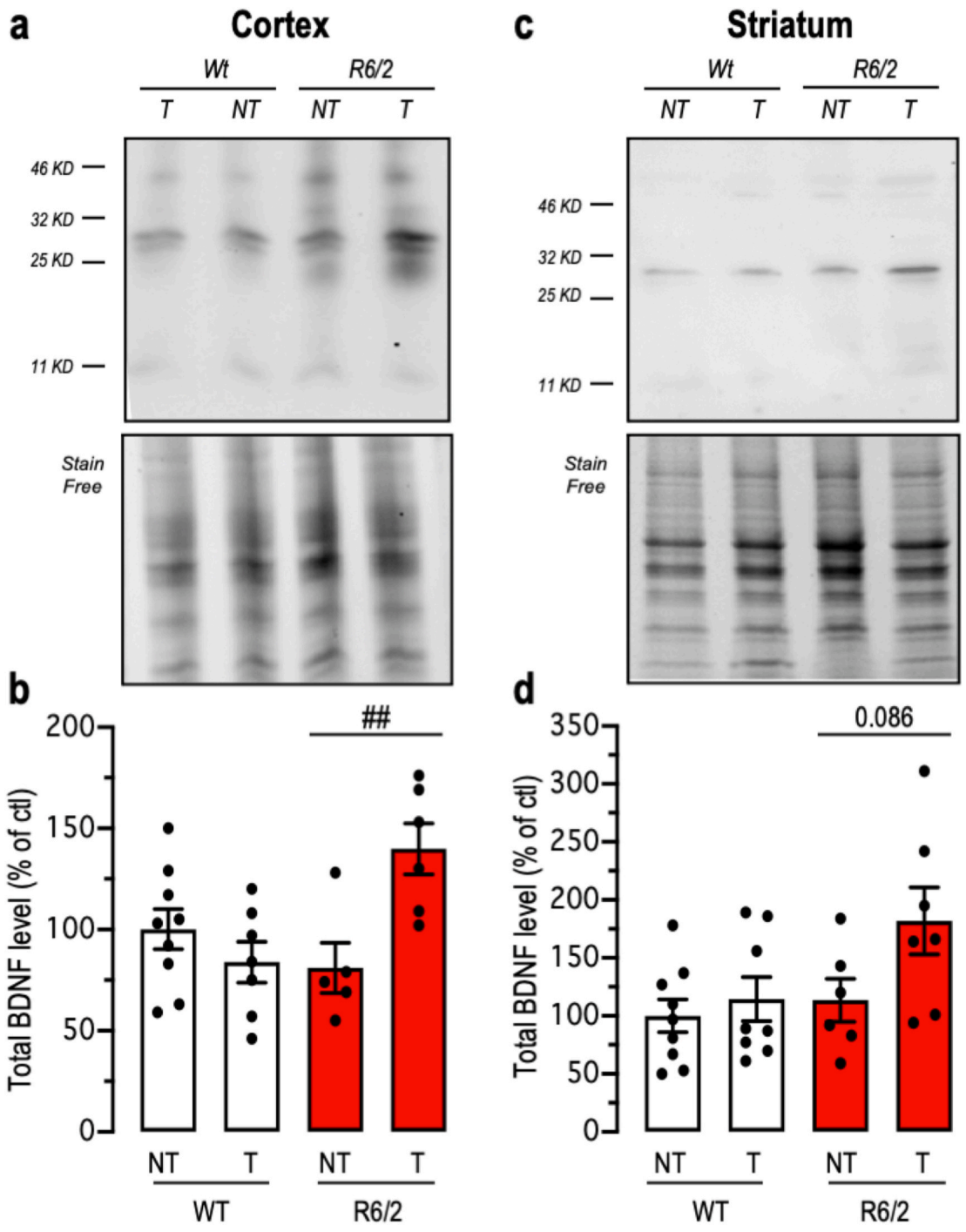

Fig. 7. Effect of training in the Hamlet on brain levels of BDNF, in the mouse cortex (a, b), and striatum (c, d). Upper panel (a, c) shows typical BDNF and stain free blots. Lower panels (b, d) show quantification in each structure. Abbreviations: WT, wild-type; NT, non-trained; T, trained. Two-way ANOVA: $F_{(1,23)} = 2.638$, $p = 0.118$ for the genotype, $F_{(1,23)} = 3.565$, $p = 0.0717$ for the training, $F_{(1,23)} = 10.87$, $p = 0.0032$ for the interaction in (b); $F_{(1,35)} = 3.31$, $p = 0.0774$ for the genotype, $F_{(1,35)} = 3.374$, $p = 0.0747$ for the training, $F_{(1,35)} = 2.881$, $p = 0.0985$ for the interaction in (d). $\#\#p < 0.01$ *vs.* NT group; Newman-Keuls test.

tested in water-deprived (WD) condition as compared to non-water-deprived (NWD) condition (Fig. 4a,c), showing that they learned the topography of the maze leading to the Drink house, during the 2-week period of free exploration of the Hamlet. V-treated R6/2 mice showed similar performances in WD or NWD condition for both errors (Fig. 4b) or latency (Fig. 4d), indicating that they did not learn the maze configuration and were unable to rapidly find the Drink house even in WD condition. P42-treated R6/2 improved their memory ability since they showed twice less errors (13 *vs.* 27 for V-treated R6/2, $p = 0.17$; Fig. 4b) and a significant diminution of the latency (Fig. 4d). These data indicated that R6/2 mice present a major deficit in topographic memory that the P42 treatment could alleviate.

Altogether, these observations in the Hamlet test showed that training is impaired in R6/2 mice after week 6 of age and that the P42 treatment preserved the level of exploration of the complex environment until week 8 of age. When mice were tested for topographic memory at week 7, R6/2 showed a major deficit that was alleviated by the P42 treatment.

3.2. Motor performances

The impact on the pathological evolution of the (V or P42) treatment and/or training or not (T or NT) in the Hamlet were analyzed on motor responses. Mice from batches 1 and 2 were tested in the Rotarod test, at weeks 7, 9, 10 and 12 (Figs. 1a and 5). As compared to control V/NT WT animals, V/NT R6/2 mice showed highly significant deficits in falling latency at all time-points measured (Fig. 5a–d). A moderate and non-significant increase in latency was observed for P42/NT mice at weeks 7 ($p = 0.13$) (Fig. 5a), but not 9, 10 and 12 (Fig. 5b,c,d). Training alone significantly improved the motor performances in V/T R6/2 mice at week 7 (Fig. 5a), and allowed a similar trend at all other time-point measured (Fig. 5b–d). However, the P42/T combination significantly improved falling latency at all time-points (Fig. 5a–d), clearly showing a potentiating effect between the peptide treatment and behavioral stimulation.

3.3. Aggregated Htt levels

As we previously reported that P42 reduced aggregate formation of polyQ-hHtt in HeLa cells (Arribat et al., 2013) and in R6/2 mice *in vivo* (Arribat et al., 2014), we examined the effect of the combined treatment and Hamlet training in R6/2 mice. Mice were sacrificed at week 11 (Fig. 1) and the levels of aggregated Htt (aHtt) analyzed by western blotting in forebrain structures (Fig. 6). In the different parts of the forebrain (hippocampus, cortex and striatum) significant effects were observed for the P42/T group. Indeed, in the hippocampus, significant group differences were observed for P42/NT mice, V/T and P42/T mice as compared with V/NT controls (Fig. 6a and b). In the cortex, the P42/T group showed significantly less aggregates than V/NT controls (Fig. 6c and d). In the striatum, a significant effect of training was noted even without P42 treatment. Notably, P42/T group showed significantly less aggregated than P42/NT group (Fig. 6e and f).

3.4. BDNF levels

We finally analyzed BDNF levels in WT and R6/2 mice, trained or not in the Hamlet. Analyses were done at week 12, thus at the very late stage of the pathology. Total BDNF was quantified by summing the bands corresponding to mature BDNF monomer, additionally to dimer and proBDNF (Fig. 7a,c). Surprisingly, we did not observe a decrease in BDNF levels in R6/2 mice in the cortex (Fig. 7a and b) or striatum (Fig. 7c and d). However, although BDNF levels were not affected by Hamlet training in WT mice, a very significant increase was measured in the cortex of R6/2 mice after training (Fig. 7a,b) and a clear trend was noted in the striatum (Fig. 7c and d).

4. Discussion

In the present study, we combined EE, using training in the Hamlet test, with the P42 peptide therapy in R6/2 mice, in order to determine whether the combination of a BDNF increase with a P42 treatment could lead to an improved therapeutic efficacy. HD pathology develops rapidly in R6/2 mice, with initial signs of motor alterations and particularly hyperactivity around 3 weeks of age, hypoactivity around 8 weeks of age and progressive rotarod deficits (Li et al., 2005). R6/2 mice show severe impairments by 8–12 weeks of age with lethality around 13–16 weeks. It is thus a very rapid disease progression and we therefore considered the early stage of the pathology at weeks <8 and late stage at weeks >8 (Fig. 1a). In terms of brain pathology, R6/2 mice show lower brain volume, mHtt aggregates and inclusions in the striatum at 3–4 weeks of age (Li et al., 2005), and alterations of neuronal activity in the firing pattern of cortico-striatal pathways (Carter et al., 1999; Cepeda et al., 2003; Rattray et al., 2013). We previously confirmed motor deficits in clasping response and rotarod performances at week 6 (Arribat et al., 2014). Moreover, we observed astroglial reaction and accumulation of mHtt aggregates throughout the cortex and striatal formation in the mice at 11 weeks of age (Arribat et al., 2014). Neurotrophic support is attenuated early in disease progression due to defects in TrkB signal transduction in striatum of R6/2 mice (Nguyen et al., 2016). The source of BDNF comes from the cortex that is transported to the striatum by corticostriatal projecting neurons. Both the level of expression and its transport are highly affected in HD (Altar et al., 1997; Ferrer et al., 2000; Zuccato et al., 2001; Gauthier et al., 2004). In HD, TrkB receptor density is lower and its signaling impaired (Ginés et al., 2010). We previously identified that P42 treatment is able to enhance TrkB protein level in the striatum, but only slightly the level of expression of BDNF in the cortex (Couly et al., 2018). Additionally, as a part of Htt protein, P42 treatment was also shown to enhance the vesicular transport along the axons (Arribat et al., 2013). This suggested that providing supplementary BDNF in addition to P42 may be beneficial. To this end, we tested in the present study the P42 treatment in EE conditions, as EE is associated with higher levels of BDNF in brain structures (Ickes et al., 2000; Mosaferi et al., 2015; Gualtieri et al., 2017). Moreover, EE has already been shown to attenuate HD symptoms in mouse models (van Dellen et al., 2000; Hockly et al., 2002). EE was induced by training the mice in the Hamlet, a powerful procedure stimulating brain plasticity and hippocampal neurogenesis (Crouzier et al., 2018).

EE was introduced between weeks 5–6 (early stage) and at weeks 8–9 (late stage). The therapeutic consequences of a combined treatments between P42 and EE were analyzed first in terms of behavioral symptoms and brain pathology, particularly regarding mHtt aggregation and BDNF expression levels. We first observed that the global activity in the Hamlet was gradually altered in R6/2 mice treated with vehicle solution. At early week 5, R6/2 mice behave like WT controls (day 1 week 5). Later on, at week 6 and throughout weeks 8–9, R6/2 activity was significantly decreased. The number of entries in each house was significantly lower for R6/2 mice except at the first day of training. Noteworthily, mice showed systemically a higher number of entries in the Run house, suggesting a preferential and beneficial impact of physical exercise in R6/2 mice. The P42 treatment, initiated just after weaning at week 4 and given daily, resulted in a significant improvement of the global activity score during the training at week 6 and 7. This improvement was observable for entries in all houses, suggesting that P42-treated R6/2 mice were globally in a better physical shape and were able to explore more the device.

R6/2 mice have been described to quickly present cognitive alterations. Since deficits in spatial learning has been observed (Lione et al., 1999), here we tested the topographic memory after training in the Hamlet of animals at 7 weeks of age when mice do not yet present motor deficits that could interfere with the memory response. Topographic memory is a more complex memory process than spatial memory, as it can be assessed in the water-maze, since it involves for the animal to mobilize not only an allocentric strategy but also an egocentric strategy (Crouzier et al., 2018). Mice were tested in normal and water-deprived conditions to find the Drink house. Both V- and P42-treated WT mice showed a significant decrease in the number of errors and latency spent to reach the Drink house. Vehicle-treated R6/2 mice did not improve their performances in WD condition and spent around 4 min to reach the Drink house, showing that they did not realize the maze topography. With P42 treatment, R6/2 mice improved their performances, particularly significant in terms of latency. These first observations on a global activity score and a cognitive response suggested that the P42 treatment resulted in delaying the pathological severity in R6/2 mice, when submitted to EE.

We then compared the impact of P42 treatment alone or in combination with EE. The motor assessment in the rotarod test performed throughout the course of the pathology (at weeks 7, 9, 10 and 12), showed that P42 or EE alone resulted in moderate increases in the rotarod score, but the P42 + EE combination allowed significant improvements of the motor performances, as compared to non-trained V-treated R6/2 animals. This was observable at all timepoints until week

12 in male mice. Noteworthily, the P42 treatment effect alone was less intense in the present study as compared with our previous report (Arribat et al., 2014). This was mainly due to the fact that we here kept mice in housing cages devoid of any enrichment routinely added in our facility. Motor symptoms therefore suggested a clear enhancement of the therapeutic efficacy for the P42 in EE, as compared to the treatment with P42 alone.

Brain pathology in HD mice first results in the accumulation of mHtt aggegates in the forebrain structures. The P42 therapy was previously reported to reduce the number, but not the size, of aHtt in the cortex and striatum, using immunohistochemical analyses (Arribat et al., 2014). We now observed in the hippocampus that the P42 treatment, EE alone or their combination resulted in significant decreases in aHtt levels. In the cortex and striatum, only the P42 + EE combination allowed significant decreases in aHtt levels, indicating that the combined therapy may have a disease-modifying effect on HD pathology progression.

Finally, we analyzed the impact of EE on BDNF contents in the R6/2 mouse brain, in the cortex and striatum. EE is known to increase BDNF levels in forebrain structures (Falkenberg et al., 1992; Bekinschtein et al., 2011) and BDNF mRNA is rapidly increased during the first week of training in Hamlet (Crouzier et al., 2020). HD is resulting from plasticity and synaptic dysfunctions associated with a deficit in BDNF levels (Baydyuk and Xu, 2014; Plotkin and Surmeier, 2015; Smith-Dijak et al., 2019) and such alterations of cortical and striatal BDNF has been described in the R6/2 mouse model (Strand et al., 2007; Couly et al., 2018). Using the same R6/2 mouse model, Nguyen et al. (2016) showed that, prior to striatal degeneration, early deficits in BDNF striatal proteins are observed, such as the activated phospho-TrkB receptor form and the downstream-regulated protein DARPP-32. In contrast, total TrkB and BDNF protein levels remained normal. Using an *in* vitro model of primary neurons cultured from R6/2 striatum, they observed that the BDNF-induced activation of TrkB was attenuated in R6/2 striatal cultures (Nguyen et al., 2016). These results confirmed that the alteration in corticostriatal neuronal activity, an early event in the disease progression, is mainly due to decreased BDNF levels associated with defects in TrkB signal transduction in the R6/2 model of HD as compared to control condition.

Since we performed the analyses late in the pathological course, we chose to analyze globally the total BDNF content in each structure by Western blot. We observed a significant increase in cortex and a trend in the striatum, close-to-significance, in R6/2 mice in enriched environment. We previously reported that a presymptomatic treatment (starting at week 3) or post-symptomatic treatment (starting at week 7) showed that the P42 treatments improved BDNF/TrkB signaling by essentially a spatio-temporal regulation of the expression of *bdnf* and *trkB* mRNAs along the corticostriatal pathways with a sustained impact on TrkB protein expression in the striatum (Couly et al., 2018). BDNF protein levels were however only marginally recovered by P42, suggesting that the peptide might incompletely restore the control of neuronal activity in the striatum. Combination with a more effective BDNF releasing therapy, as could be achieved here with EE, confirmed this hypothesis. Indeed, associated with this enhancement of BDNF protein level, we observed in these conditions a more efficient BDNF/TrkB signaling pathway, which drives a significant protection regarding motor performances and pathological readouts, *e.g.*, mHtt aggregation or memory tasks. Increases in cortical and striatal BDNF protein level could be achieved by different means. For instance, long-term treatment with doxycycline was shown to improve motor response in R6/2 mice and to mitigate microglial reaction by enhancing CREB and BDNF protein expression (Paldino et al., 2019). The same authors also systemically administered recombinant BDNF and observed particularly that it increased the level of phosphorylated CREB protein, a sign for enhanced neuronal activity (Paldino et al., 2020). As BDNF is involved in numerous physiopathological conditions, including depression or memory alterations for instance, numerous BDNF mimetics or releasing agents are currently under investigation. Such agents may provide an alternative way to direct application of BDNF that present limited therapeutic opportunity (Connor et al., 2016).

Table 2
Schematic summary of the observed effects of P42 + EE combination on behavioral and biochemical measures.

Effect	P42	EE	P42 + EE
(**A**) Rotarod score			
at week 7	+	++	++
at week 9	–	+	++
at week 10	–	+	++
at week 12	–	–	++
(**B**) Aggregated HTT levels			
Hippocampus	++	++	++
Cortex	–	–	++
Striatum	–	–	++

Abbreviations: EE, enriched environment; -, no effect; +, tendency to improve; ++, significant improvement vs V-treated NT mice. from data in Figs. 5–6.

5. Conclusions

We combined a peptide treatment, using the Htt fragment peptide P42, and EE in R6/2 mice developing rapidly the HD pathology. We showed that the combination allowed an over significant period of time (2 weeks, in a mouse model where the pathology develops over 13 weeks) to delay the intensity of the motor and cognitive impairments and brain pathology (mHtt aggegates). To summarize our findings, Table 2 synthetized the effects of P42, EE and their combination, as observed in Figs. 5–6, on a behavioral impairment (Rotarod) and a pathological measures (aggregated HTT levels). In the rotarod (Table 2A), P42 alone was effective at week 7 only, EE at weeks 7–10 and only the combination led to an augmented effect at all weeks and significant throughout weeks 7–12. For aggregated HTT levels (Table 2B), significant effects of P42-EE combination were identified in the cortex and striatum, again showing that the combination led to an augmented effect. Moreover, it appeared that EE allowed to markedly increase BDNF levels in the cortex and striatum and therefore, combined to the demonstrated effect of P42 on TrkB expression and vesicular trafficking (Arribat et al., 2013; Couly et al., 2018) to sustain efficiently the cortico-striatal neuronal activity in HD mice. Altogether these results suggest that targeting BDNF/TrkB pathway in HD is an effective therapeutic solution, not only through BDNF increase, but also through the enhancement of striatal TrkB protein level of expression. Therefore, as shown in this report, combination of P42 treatment in an enriched environment to boost BDNF brain concentration could lead to a viable option to markedly delay HD symptoms.

CRediT authorship contribution statement

Simon Couly: Conceptualization, Formal analysis, Investigation, Methodology, Writing - original draft, Writing - review & editing. **Allison Carles:** Investigation. **Morgane Denus:** Investigation. **Lorraine Benigno-Anton:** Resources. **Florence Maschat:** Conceptualization, Formal analysis, Funding acquisition, Methodology, Project administration, Writing - original draft, Writing - review & editing. **Tangui Maurice:** Conceptualization, Formal analysis, Methodology, Writing - original draft, Writing - review & editing.

Declaration of competing interest

Dr. Maschat has a patent PCT/FR 2012/050809 issued related to P42 therapy. Dr. Maurice has a patent FR15 57093, Ext. WO 2017/017010, describing the Hamlet test, licensed to Viewpoint. The other authors declare no competing interest.

Acknowledgements

We thank Jean-Charles Liévens (MMDN) and Elsa Compte (Medesis Pharma) for their helpful discussions and comments on the manuscript. We thank Bénédicte Fauvel (SATT AxLR) for support. We thank the Genomix qPHD platform, the CECEMA-UM animal facility of the Montpellier University, and the MRI imaging facility.

Appendix A. Supplementary data

Supplementary data to this article can be found online at https://doi.org/10.1016/j.neuropharm.2021.108467.

Funding

This work has been supported by Agence Nationale de la Recherche (ANR-12-EMMA-0013; ANR-14-CE13-0035). This project also received financial support from SATT AxLR, the Occitanie Region, Montpellier Méditerranée Métropole and Feder funds.

References

Altar, C.A., Cai, N., Bliven, T., Juhasz, M., Conner, J.M., Acheson, A.L., Lindsay, R.M., Wiegand, S.J., 1997. Anterograde transport of brain-derived neurotrophic factor and its role in the brain. Nature 389, 856–860. https://doi.org/10.1038/39885.

Apostol, B.L., Simmons, D.A., Zuccato, C., Illes, K., Pallos, J., Casale, M., Conforti, P., Ramos, C., Roarke, M., Kathuria, S., Cattaneo, E., Marsh, J.L., Thompson, L.M., 2008. CEP-1347 reduces mutant huntingtin-associated neurotoxicity and restores BDNF levels in R6/2 mice. Mol. Cell. Neurosci. 39, 8–20. https://doi.org/10.1016/j.mcn.2008.04.007.

Arribat, Y., Bonneaud, N., Talmat-Amar, Y., Layalle, S., Parmentier, M.L., Maschat, F., 2013. A huntingtin peptide inhibits polyQ-huntingtin associated defects. PloS One 8, e68775. https://doi.org/10.1371/journal.pone.0068775.

Arribat, Y., Talmat-Amar, Y., Paucard, A., Lesport, P., Bonneaud, N., Bauer, C., Bec, N., Parmentier, M.L., Benigno, L., Larroque, C., Maurel, P., Maschat, F., 2014. Systemic delivery of P42 peptide: a new weapon to fight Huntington's disease. Acta Neuropathol. Commun. 2, 86. https://doi.org/10.1186/s40478-014-0086-x.

Bates, G.P., Dorsey, R., Gusella, J.F., Hayden, M.R., Kay, C., Leavitt, B.R., Nance, M., Ross, C.A., Scahill, R.I., Wetzel, R., Wild, E.J., Tabrizi, S.J., 2015. Huntington disease. Nat. Rev. Dis. Primers 1, 15005. https://doi.org/10.1038/nrdp.2015.5.

Baydyuk, M., Xu, B., 2014. BDNF signaling and survival of striatal neurons. Front. Cell. Neurosci. 8, 254. https://doi.org/10.3389/fncel.2014.00254.

Bekinschtein, P., Oomen, C.A., Saksida, L.M., Bussey, T.J., 2011. Effects of environmental enrichment and voluntary exercise on neurogenesis, learning and memory, and pattern separation: BDNF as a critical variable? Semin. Cell Dev. Biol. 22, 536–542. https://doi.org/10.1016/j.semcdb.2011.07.002.

Bobrowska, A., Paganetti, P., Matthias, P., Bates, G.P., 2011. Hdac6 knock-out increases tubulin acetylation but does not modify disease progression in the R6/2 mouse model of Huntington's disease. PloS One 6, e20696. https://doi.org/10.1371/journal.pone.0020696.

Canals, J.M., Pineda, J.R., Torres-Peraza, J.F., Bosch, M., Martín-Ibañez, R., Muñoz, M.T., Mengod, G., Ernfors, P., Alberch, J., 2004. Brain-derived neurotrophic factor regulates the onset and severity of motor dysfunction associated with enkephalinergic neuronal degeneration in Huntington's disease. J. Neurosci. 24 https://doi.org/10.1523/jneurosci.1197-04.2004, 7727-39.

Carter, R.J., Lione, L.A., Humby, T., Mangiarini, L., Mahal, A., Bates, G.P., Dunnet, S.B., Morton, A.J., 1999. Characterization of progressive motor deficits in mice transgenic for the human Huntington's disease mutation. J. Neurosci. 19, 3248–3257. https://doi.org/10.1523/jneurosci.19-08-03248.1999.

Cepeda, C., Hurst, R.S., Calvert, C.R., Hernández-Echeagaray, E., Nguyen, O.K., Jocoy, E., Christian, L.J., Ariano, M.A., Levine, M.S., 2003. Transient and progressive electrophysiological alterations in the corticostriatal pathway in a mouse model of Huntington's disease. J. Neurosci. 23 https://doi.org/10.1523/jneurosci.23-03-00961.2003, 961-9.

Connor, B., Sun, Y., von Hieber, D., Tang, S.K., Jones, K.S., Maucksch, C., 2016. AAV1/2-mediated BDNF gene therapy in a transgenic rat model of Huntington's disease. Gene Ther. 23, 283–295. https://doi.org/10.1038/gt.2015.113.

Couly, S., Paucard, A., Bonneaud, N., Maurice, T., Benigno, L., Jourdan, C., Cohen-Solal, C., Vignes, M., Maschat, F., 2018. Improvement of BDNF signalling by P42 peptide in Huntington's disease. Hum. Mol. Genet. 27, 3012–3028. https://doi.org/10.1093/hmg/ddy207.

Crouzier, L., Couly, S., Roques, C., Peter, C., Belkhiter, R., Arguel Jacquemin, M., Bonetto, A., Delprat, B., Maurice, T., 2020. Sigma-1 ($\tilde{I}f_1$) receptor activity is necessary for physiological brain plasticity in mice. Eur. Neuropsychopharmacol 39, 29–45. https://doi.org/10.1016/j.euroneuro.2020.08.010.

Crouzier, L., Gilabert, D., Rossel, M., Trousse, F., Maurice, T., 2018. Topographical memory analyzed in mice using the Hamlet test, a novel complex maze. Neurobiol. Learn. Mem. 149, 118–134. https://doi.org/10.1016/j.nlm.2018.02.014.

Crouzier, L., Maurice, T., 2018. Assessment of topographic memory in mice in a complex environment using the Hamlet test. Curr. Protoc. Mouse Biol. 8, e43. https://doi.org/10.1002/cpmo.43.

Dorsey, E.R., Beck, C.A., Darwin, K., Nichols, P., Brocht, A.F., Biglan, K.M., Shoulson, I., Huntington Study Group Cohort Investigators, 2013. Natural history of Huntington disease. JAMA Neurol 70, 1520–1530. https://doi.org/10.1001/jamaneurol.2013.4408.

Falkenberg, T., Mohammed, A.K., Henriksson, B., Persson, H., Winblad, B., Lindefors, N., 1992. Increased expression of brain-derived neurotrophic factor mRNA in rat hippocampus is associated with improved spatial memory and enriched environment. Neurosci. Lett. 138 https://doi.org/10.1016/0304-3940(92)90494-r, 153-6.

Ferrer, I., Goutan, E., Marín, C., Rey, M.J., Ribalta, T., 2000. Brain-derived neurotrophic factor in Huntington disease. Brain Res. 866, 257–261. https://doi.org/10.1016/s0006-8993(00)02237-x.

Gauthier, L.R., Charrin, B.C., Borrell-Pagès, M., Dompierre, J.P., Rangone, H., Cordelières, F.P., De Mey, J., MacDonald, M.E., Lessmann, V., Humbert, S., Saudou, F., 2004. Huntingtin controls neurotrophic support and survival of neurons by enhancing BDNF vesicular transport along microtubules. Cell 118, 127–138. https://doi.org/10.1016/j.cell.2004.06.018.

Gharami, K., Xie, Y., An, J.J., Tonegawa, S., Xu, B., 2008. Brain-derived neurotrophic factor over-expression in the forebrain ameliorates Huntington's disease phenotypes in mice. J. Neurochem. 105 https://doi.org/10.1111/j.1471-4159.2007.05137.x, 369-79.

Gilda, J.E., Gomes, A.V., 2013. Stain-Free total protein staining is a superior loading control to $\tilde{I}^2$-actin for Western blots. Anal. Biochem. 440, 186–188. https://doi.org/10.1016/j.ab.2013.05.027.

Ginés, S., Bosch, M., Marco, S., Gavaldà, N., Díaz-Hernández, M., Lucas, J.J., Canals, J. M., Alberch, J., 2006. Reduced expression of the TrkB receptor in Huntington's disease mouse models and in human brain. Eur. J. Neurosci. 23, 49–58. https://doi.org/10.1111/j.1460-9568.2006.04590.x.

Ginés, S., Paoletti, P., Alberch, J., 2010. Impaired TrkB-mediated ERK1/2 activation in Huntington disease knock-in striatal cells involves reduced p52/p46 Shc expression. J. Biol. Chem. 285, 21537–21548. https://doi.org/10.1074/jbc.M109.084202.

Giralt, A., Rodrigo, T., Martín, E.D., Gonzalez, J.R., Milà, M., Ceña, V., 2009. Brain-derived neurotrophic factor modulates the severity of cognitive alterations induced by mutant huntingtin: involvement of phospholipase$\tilde{C}\tilde{I}^3$ activity and glutamate receptor expression. Neuroscience 158, 1234–1250. https://doi.org/10.1016/j.neuroscience.2008.11.024.

Gualtieri, F., Brégère, C., Laws, G.C., Armstrong, E.A., Wylie, N.J., Moxham, T.T., Guzman, R., Boswell, T., Smulders, T.V., 2017. Effects of environmental enrichment on doublecortin and BDNF expression along the dorso-ventral axis of the dentate gyrus. Front. Neurosci. 11, 488. https://doi.org/10.3389/fnins.2017.00488.

Guilarte, T.R., Toscano, C.D., McGlothan, J.L., Weaver, S.A., 2003. Environmental enrichment reverses cognitive and molecular deficits induced by developmental lead exposure. Ann. Neurol. 53, 50–56. https://doi.org/10.1002/ana.10399.

Gürtler, A., Kunz, N., Gomolka, M., Hornhardt, S., Friedl, A.A., McDonald, K., Kohn, J.E., Posch, A., 2013. Stain-Free technology as a normalization tool in Western blot analysis. Anal. Biochem. 433, 105–111. https://doi.org/10.1016/j.ab.2012.10.010.

Hockly, E., Cordery, P.M., Woodman, B., Mahal, A., van Dellen, A., Blakemore, C., Lewis, C.M., Hannan, A.J., Bates, G.P., 2002. Environmental enrichment slows disease progression in R6/2 Huntington's disease mice. Ann. Neurol. 51, 235–242. https://doi.org/10.1002/ana.10094.

Huntington, G., 1872. On chorea. Medical and Surgical Reporter of Philadelphia 26, 317–321.

Ickes, B.R., Pham, T.M., Sanders, L.A., Albeck, D.S., Mohammed, A.H., Granholm, A.C., 2000. Long-term environmental enrichment leads to regional increases in neurotrophin levels in rat brain. Exp. Neurol. 164, 45–52. https://doi.org/10.1006/exnr.2000.7415.

Kilkenny, C., Browne, W., Cuthill, I.C., Emerson, M., Altman, D.G., Nc3Rs Reporting Guidelines Working Group, 2010. Animal research: reporting in vivo experiments: the ARRIVE guidelines. Br. J. Pharmacol. 160, 1577–1579. https://doi.org/10.1111/j.1476-5381.2010.00872.x.

Li, J.Y., Popovic, N., Brundin, P., 2005. The use of the R6 transgenic mouse models of Huntington's disease in attempts to develop novel therapeutic strategies. NeuroRx 2. https://doi.org/10.1602/neurorx.2.3.447, 447-64.

Lione, L.A., Carter, R.J., Hunt, M.J., Bates, G.P., Morton, A.J., Dunnett, S.B., 1999. Selective discrimination learning impairments in mice expressing the human Huntington's disease mutation. J. Neurosci. 19, 10428–10437. https://doi.org/10.1523/JNEUROSCI.19-23-10428.1999.

Luthi-Carter, R., Hanson, S.A., Strand, A.D., Bergstrom, D.A., Chun, W., Peters, N.L., Woods, A.M., Chan, E.Y., Kooperberg, C., Krainc, D., Young, A.B., Tapscott, S.J., Olson, J.M., 2002. Dysregulation of gene expression in the R6/2 model of polyglutamine disease: parallel changes in muscle and brain. Hum. Mol. Genet. 11, 1911–1926. https://doi.org/10.1093/hmg/11.17.1911.

Mosaferi, B., Babri, S., Mohaddes, G., Khamnei, S., Mesgari, M., 2015. Post-weaning environmental enrichment improves BDNF response of adult male rats. Int. J. Dev. Neurosci. 46, 108–114. https://doi.org/10.1016/j.ijdevneu.2015.07.008.

Mouri, A., Diat, O., El Ghzaoui, A., Ly, I., Dorandeu, C., Maurel, J.C., 2015. Development of pharmaceutical clear gel based on Peceol®, lecithin, ethanol and water: physicochemical characterization and stability study. J. Colloid Interface Sci. 457, 152–161. https://doi.org/10.1016/j.jcis.2015.06.010.

Mouri, A., Diat, O., Lerner, D.A., El Ghzaoui, A., Ajovalasit, A., Dorandeu, C., Maurel, J. C., Devoisselle, J.M., Legrand, P., 2014. Water solubilization capacity of pharmaceutical microemulsions based on Peceol®, lecithin and ethanol. Int. J. Pharm. 475, 324–334. https://doi.org/10.1016/j.ijpharm.2014.07.018.

Mouri, A., Legrand, P., El Ghzaoui, A., Dorandeu, C., Maurel, J.C., Devoisselle, J.M., 2016. Formulation, physicochemical characterization and stability study of lithium-loaded microemulsion system. Int. J. Pharm. 502, 117–124. https://doi.org/10.1016/j.ijpharm.2016.01.072.

Nguyen, K.Q., Rymar, V.V., Sadikot, A.F., 2016. Impaired TtrkbB signaling underlies reduced BDNF-mediated trophic support of striatal neurons in the R6/2 mouse model of Huntington's disease. Front. Cell. Neurosci. 10, 37. https://doi.org/10.3389/fncel.2016.00037.

Orr, H.T., Chung, M.Y., Banfi, S., Kwiatkowski Jr., T.J., Servadio, A., Beaudet, A.L., McCall, A.E., Duvick, L.A., Ranum, L.P., Zoghbi, H.Y., 1993. Expansion of an unstable trinucleotide CAG repeat in spinocerebellar ataxia type 1. Nat. Genet. 4, 221–226. https://doi.org/10.1038/ng0793-221.

Paldino, E., Balducci, C., La Vitola, P., Artioli, L., D'Angelo, V., Giampà, C., 2020. Neuroprotective effects of doxycycline in the R6/2 mouse model of Huntington's disease. Mol. Neurobiol. 57, 1889–1903. https://doi.org/10.1007/s12035-019-01847-8.

Paldino, E., Giampà, C., Montagna, E., Angeloni, C., Fusco, F.R., 2019. Modulation of phospho-CREB by systemically administered recombinant BDNF in the hippocampus of the R6/2 mouse model of Huntington's dsease. Neurosci. J. 2019 8363274. https://doi.org/10.1155/2019/8363274.

Plotkin, J.L., Day, M., Peterson, J.D., Xie, Z., Kress, G.J., Rafalovich, I., Kondapalli, J., Gertler, T.S., Flajolet, M., Greengard, P., Stavarache, M., Kaplitt, M.G., Rosinski, J., Cha, C.S., Surmeier, D.J., 2014. Impaired TrkB receptor signaling underlies corticostriatal dysfunction in Huntington's disease. Neuron 83, 178–188. https://doi.org/10.1016/j.neuron.2014.05.032.

Plotkin, J.L., Surmeier, D.J., 2015. Corticostriatal synaptic adaptations in Huntington's disease. Curr. Opin. Neurobiol. 33, 53–62. https://doi.org/10.1016/j.conb.2015.01.020.

Rattray, I., Smith, E., Gale, R., Matsumoto, K., Bates, G.P., Modo, M., 2013. Correlations of behavioral deficits with brain pathology assessed through longitudinal MRI and histopathology in the R6/2 mouse model of HD. PloS One 8, e60012. https://doi.org/10.1371/journal.pone.0060012.

Reijonen, S., Putkonen, N., Nørremølle, A., Lindholm, D., Korhonen, L., 2008. Inhibition of endoplasmic reticulum stress counteracts neuronal cell death and protein aggregation caused by N-terminal mutant huntingtin proteins. Exp. Cell Res. 314, 950–960. https://doi.org/10.1016/j.yexcr.2007.12.025.

Simmons, D.A., Belichenko, N.P., Yang, T., Condon, C., Monbureau, M., Shamloo, M., Jing, D., Massa, S.M., Longo, F.M., 2013. A small molecule TrkB ligand reduces motor impairment and neuropathology in R6/2 and BACHD mouse models of Huntington's disease. J. Neurosci. 33 https://doi.org/10.1523/jneurosci.1310-13.2013, 18712-27.

Smith-Dijak, A.I., Sepers, M.D., Raymond, L.A., 2019. Alterations in synaptic function and plasticity in Huntington disease. J. Neurochem. 150, 346–365. https://doi.org/10.1111/jnc.14723.

Spires, T.L., Grote, H.E., Garry, S., Cordery, P.M., Van Dellen, A., Blakemore, C., Hannan, A.J., 2004. Dendritic spine pathology and deficits in experience-dependent dendritic plasticity in R6/1 Huntington's disease transgenic mice. Eur. J. Neurosci. 19, 2799–2807. https://doi.org/10.1111/j.0953-816X.2004.03374.x.

Strand, A.D., Baquet, Z.C., Aragaki, A.K., Holmans, P., Yang, L., Cleren, C., Beal, M.F., Jones, L., Kooperberg, C., Olson, J.M., Jones, K.R., 2007. Expression profiling of Huntington's disease models suggests that brain-derived neurotrophic factor depletion plays a major role in striatal degeneration. J. Neurosci. 27, 11758–11768. https://doi.org/10.1523/jneurosci.2461-07.2007.

van Dellen, A., Blakemore, C., Deacon, R., York, D., Hannan, A.J., 2000. Delaying the onset of Huntington's in mice. Nature 404, 721–722. https://doi.org/10.1038/35008142. PMID: 10783874.

Young, D., Lawlor, P.A., Leone, P., Dragunow, M., During, M.J., 1999. Environmental enrichment inhibits spontaneous apoptosis, prevents seizures and is neuroprotective. Nat. Med. 5, 448–453. https://doi.org/10.1038/7449.

Zhao, L.R., Risedal, A., Wojcik, A., Hejzlar, J., Johansson, B.B., Kokaia, Z., 2001. Enriched environment influences brain-derived neurotrophic factor levels in rat forebrain after focal stroke. Neurosci. Lett. 305, 169–172. https://doi.org/10.1016/s0304-3940(01)01837-7.

Zuccato, C., Ciammola, A., Rigamonti, D., Leavitt, B.R., Goffredo, D., Conti, L., MacDonald, M.E., Friedlander, R.M., Silani, V., Hayden, M.R., Timmusk, T., Sipione, S., Cattaneo, E., 2001. Loss of huntingtin-mediated BDNF gene transcription in Huntington's disease. Science 293, 493–498. https://doi.org/10.1126/science.1059581.